Technical Report

TR-05-18

Pressure tests of two KBS-3 canister mock-ups

Karl-Fredrik Nilsson, Frantisek Lofaj
European Commission, DG-JRC, Institute for Energy,
Petten, The Netherlands

Martin Burström
MABU Consulting AB

Claes-Göran Andersson
Svensk Kärnbränslehantering AB

Svensk Kärnbränslehantering AB
Swedish Nuclear Fuel
and Waste Management Co
Box 5864
SE-102 40 Stockholm Sweden
Tel 08-459 84 00
+46 8 459 84 00
Fax 08-661 57 19
+46 8 661 57 19

Pressure tests of two KBS-3 canister mock-ups

Karl-Fredrik Nilsson, Frantisek Lofaj
European Commission, DG-JRC, Institute for Energy,
Petten, The Netherlands

Martin Burström
MABU Consulting AB

Claes-Göran Andersson
Svensk Kärnbränslehantering AB

Executive summary

The Swedish concept for geological disposal of spent nuclear fuel, the so-called KBS-3 concept, relies on a multibarrier system with the copper/cast iron canister as the first barrier. The canister is designed to retain its integrity for at least 100,000 years, which means that future glaciations need to be considered. A 3 km thick ice block together with hydrostatic pressure from groundwater and swelling of the buffer material would produce hydrostatic compressive stresses of maximum 44 MPa (440 bar). Although the canister is loaded globally in compression, tensile stresses develop at fuel channel surface with increasing load. Tensile tests of the insert material in the development phase of the KBS-3 canister indicated a large scatter and relatively low values of the inserts' ductility. An important issue was whether this could lead to mechanical failure of canisters at the 44 MPa iso-static load either by plastic collapse or fracture from the defects in the regions with tensile stresses.

SKB therefore initiated a project together with the European commission's Joint Research Centre (JRC) Institute of Energy in Petten and a number of Swedish partners to evaluate the probability of mechanical failure during glaciation. Three inserts manufactured by different Swedish foundries and referred to as I24, I25 and I26 were used in the project. A large statistical test programme was developed to determine statistical distributions of various material parameters and defect distributions. These data were subsequently used in probabilistic analysis to determine the probability for local plastic collapse or fracture. The main conclusion was that the failure probability is extremely low at the design load (44 MPa) provided some basic geometrical requirements are fulfilled.

In parallel to the statistical test programme and the associated analysis, the group decided also to perform two pressure tests of canister mock-ups to demonstrate the actual safety margins. The fractographic and radiographic investigations of tensile specimens indicate that the low ductility and its scatter are caused by a combination of casting defects and microstructrual inhomogeneities. These findings suggest that the same type of defects could also induce failure in a large component of the same material and that the fracture load for a canister could be reduced by the so-called size effect (i.e. the probability of having a critical defect increases with the increasing material volume) and as a consequence the failure load will be further reduced. Two mock-ups representative of a complete KBS-3 canister were therefore designed with inserts from I26 and I24 respectively and loaded to high hydrostatic pressure in a cold isostatic press (CIP) to determine the failure load and failure mechanism.

The first mock-up, manufactured from the I26 insert, was loaded to 130 MPa. At this load the canister had undergone plastic deformation but retained its overall integrity. A detailed experimental post-test analysis programme indicated that some defects had grown up to 10 mm in stable tearing but there were no through-wall cracks. The second mock-up, manufactured from insert I24, was loaded to 139 MPa when it failed by plastic collapse. The main outcome was that these two tests demonstrated large safety margins (factor 3) even for the extreme pressure that could occur during glaciation. When it eventually fails, plastic collapse is more likely than fracture from casting defects. Through-wall fracture from defects is extremely unlikely because of the compressive stresses and the material's inherent crack growth resistance. These findings are also in good agreement with FE-element analyses.

Contents

1 Introduction

The Swedish copper/cast iron canister for deep disposal of spent nuclear fuel, Figure 1-1, is designed to retain its integrity for 100,000 years, which means that future glaciations need to be considered. The largest design load is hydrostatic pressure from groundwater and swelling of the buffer material and a 3 km ice block resulting in a total external pressure of 44 MPa (440 bar) /1/. Although the canister is loaded globally in compression, tensile stresses develop at fuel channel surface with increasing load /2/. Tensile tests of the insert material in the development phase indicated a large scatter and relatively low values of the inserts' ductility /3, 4/. An important issue was then whether this could lead to unacceptable failure probabilities of canisters at the 44 MPa iso-static load. SKB therefore initiated a project together with the European commission's Joint Research Centre (JRC) Institute of Energy in Petten and a number of Swedish partners to ensure sufficiently low probability for mechanical failure during glaciation. Three inserts manufactured by different Swedish foundries and referred to as I24, I25 and I26 were used in the project. A large statistical test programme was developed to determine statistical distributions of various material parameters and defect distributions. Figure 1-2 illustrates variation in elongation after fracture between these inserts and at different locations /5/. These data were subsequently used in probabilistic analysis to determine the probability for local plastic collapse or fracture. The main conclusion was that failure probability is extremely low at the design load (44 MPa) provided some basic geometrical requirements are fulfilled /6, 7, 8, 2/.

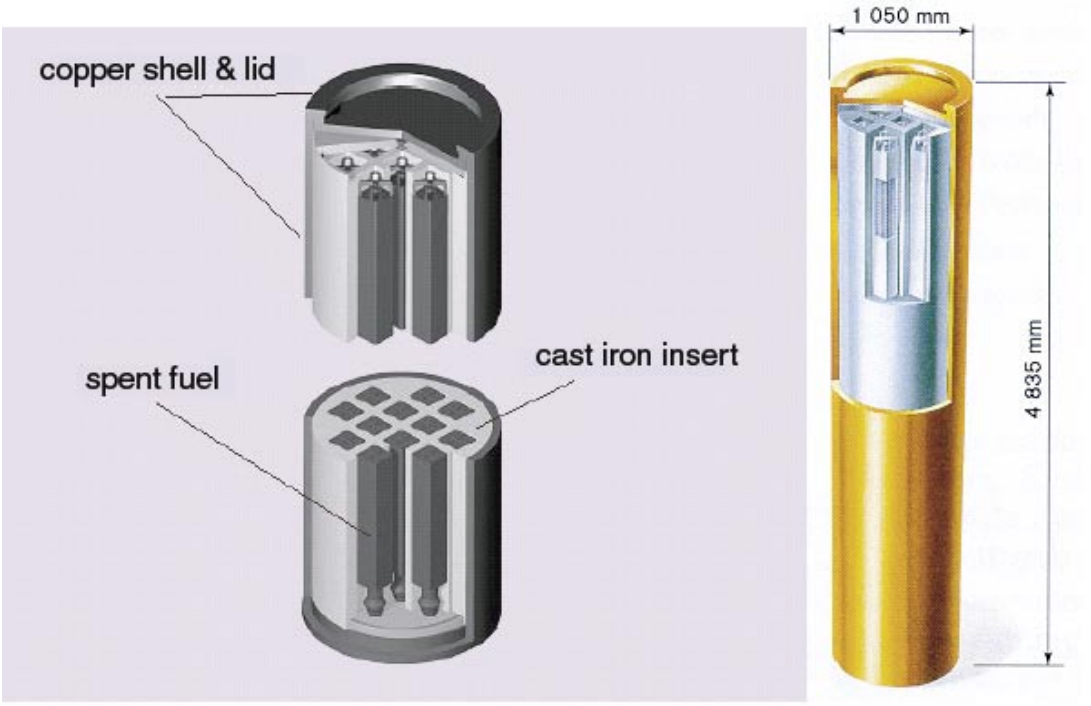

Figure 1-1. *The Swedish KBS-3 copper/cast iron canister for spent fuel.*

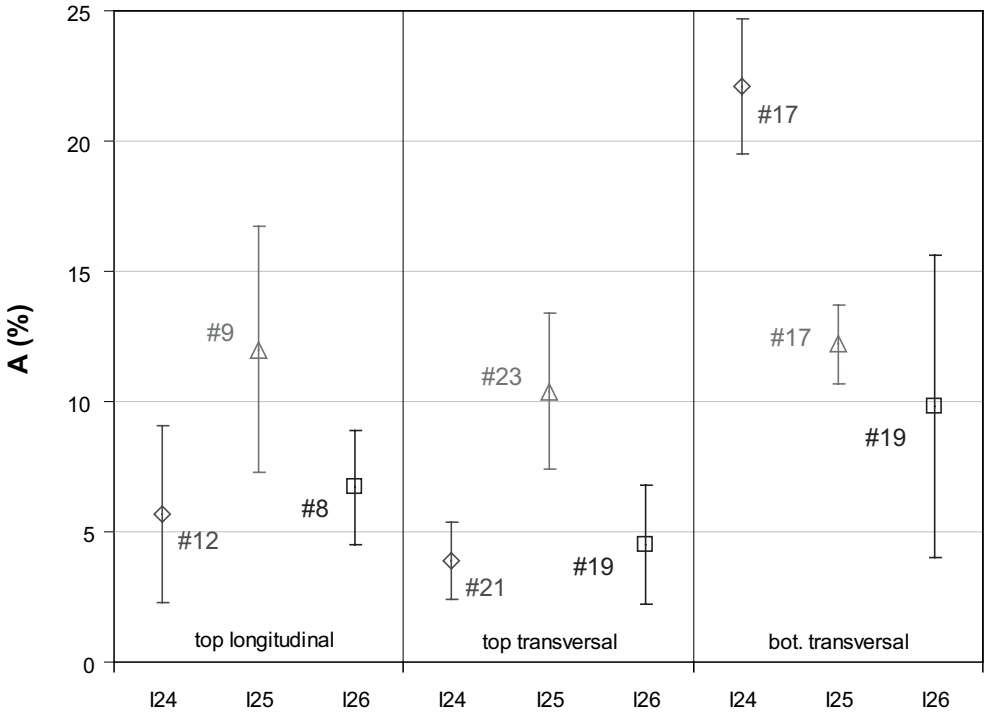

Figure 1-2. *Mean elongation after fracture for inserts I24, I25 and I26. The error bars show standard deviation and the hatches indicate the number of specimens for each data set.*

Figure 1-3 is a schematic illustration of the plastic deformation plotted against applied load up to global plastic collapse for different scenarios. The worst case would be brittle and unstable fracture from a large defect. If a cracks starts to propagate when the deformation is plastic then it is likely that further crack growth is by a stable tearing mechanism. Depending on the loading and material properties a stable tearing crack may arrest or become critical.

Although the predicted failure probabilities are very low, it is clearly of interest to demonstrate these margins by large-scale tests. The analyses mentioned above were based on local failure criteria for plastic collapse and initiation of crack growth, whereas actual failure of the canisters is more likely to be controlled by global failure modes. The safety margins are therefore in reality probably even larger and the failure probabilities lower than the predictions. On the other hand the low ductility in the tensile tests was mainly caused by slag defects. The probability for having large defects increases with the material volume, which may lead to an apparent lower fracture resistance for a large component (the so-called size effect). To verify the safety margins and ensure that there would be no major effects that are not accounted for in the analyses, two large-scale tests of mock-ups loaded in isostatic compression were performed. Large-scale tests are needed because the tests cannot be properly scaled due to plastic and large deformations. On the other hand, weight and size restrictions for test facilities require that the mock-up is smaller than the actual canister but that major features are accounted for. The report describes the engineering design of the two mock-ups, their testing and the main results.

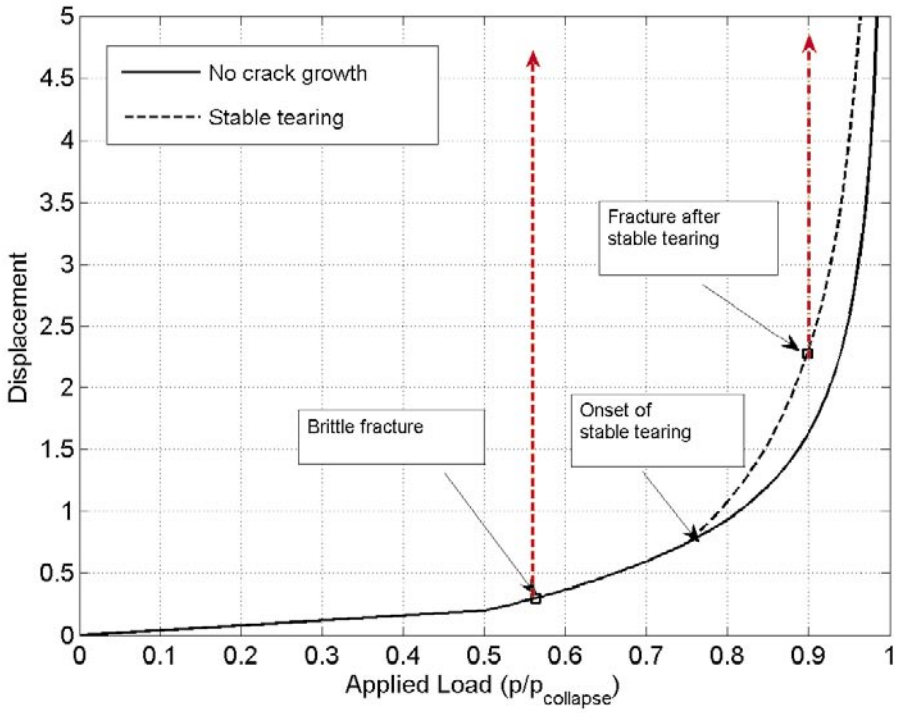

Figure 1-3. *Schematic illustration of load-displacement until plastic collapse with brittle fracture and onset of stable tearing. The dashed arrows indicate fracture by brittle fracture and after some stable tearing.*

2 Component design and assembly

The two pressure test mock-ups were designed to be as representative as possible for the KBS-3 copper/cast iron canister but with the restriction that its weight did not exceed 5 tons.

The mock-ups were made from the following parts, which had been manufactured as part of the KBS-3 development programme:

- Inserts of length 700 mm and diameter 948 mm, cut from the manufactured insert with SKB reference number I26 (Mock-up #1) and I24 (Mock-up #2). The insert design is for BWR type with twelve quadratic shaped channels, each containing a steel tube with thickness 10 mm with outer and inner dimension of 180×180 and 160×160 mm respectively.
- Copper tube with inner diameter, 952 mm, length 948 mm and thickness 50 mm, taken from material with SKB reference number T18 and T35 for Mock-up #1 and #2 respectively.
- Two copper lids from material with SKB reference numbers TX63 and TX64 (Mock-up #1) and TX119 and TX122 (Mock-up #2).
- Two 48 mm thick steel plates positioned between insert and lid at each end. The same steel plates were used for both mock-ups.

A schematic drawing of the mock-up is shown in Figure 2-1. The machining of the parts and their assembly was done by Saltängens Mekaniska Verkstad in Sweden. Figure 2-2a shows the cast iron insert, copper tube and steel plates and a detail of the copper lid for Mock-up #1. The complete KBS-3 canister has a length of almost five meters, the lids are welded to the copper tube and the bottom part of the insert is homogeneous as indicated in Figure 1-1, which provides a stiffening effect at the ends of the canister. Since the mock-up is substantially shorter than a full size KBS-3 canister, the “end effects” would be larger if the same design were used at the ends. Hence to alleviate the end-effects and allow disassembly of the mock-up after the test, the lids were attached to the both ends of the insert by one large bolt and the lid to the tube by 16 smaller bolts. Three O-rings (seen in Figure 2-2b) were attached to the lid to ensure tightness between lid and tube. The total length and weight of each mock-up were 1,050 mm and 5 tons respectively. Figure 2-3a shows the insert lowered into the copper tube and Figure 2-3b shows the assembled Mock-up #1. A rectangular pattern was machined into the copper tube for Mock-up #1 as seen in Figures 2-3a and 2-3b. The purpose of this was to better assess by visual inspection any large plastic deformations between pressure cycles. For Mock-up #2 this surface machining was not done.

The insert Mock-up #1 was cut from the segment with the largest defect indications from ultra-sound [1]. The ultra-sound investigation could not size the defects. Casting defects were, however, observed at the end surfaces of the mock-up insert. A typical casting defect with a size of thumbnail can be seen in Figure 2-4. Another important manufacturing deviation was that the fuel bundle channels had an off-set of 12 mm from its assumed symmetric location. As a consequence the wall thickness between the outer surface and the corner of the fuel channel varied from 22 to 44 mm at the locations indicated in Figure 2-5. This off-set will

[1] G Emilsson, 2003. Förslag på kapning av insats I26, CSM Materialteknik, Teknisk Rapport TEK03-0458.

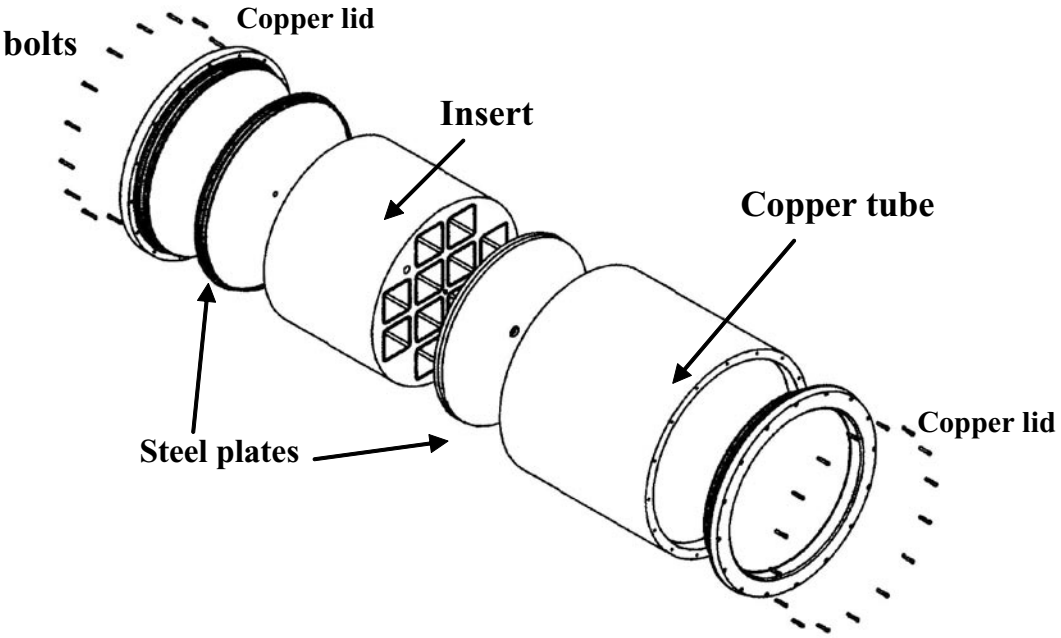

Figure 2-1. *Schematic drawing of mock-up (to be done).*

a) *b)*

Figure 2-2. *a) Cast iron insert and copper tube cut to specified dimensions and machined before assembly b) detail of copper lid with O-rings.*

a) *b)*

Figure 2-3. *a) Cast iron insert being inserted into the copper tube and b) assembled mock-up.*

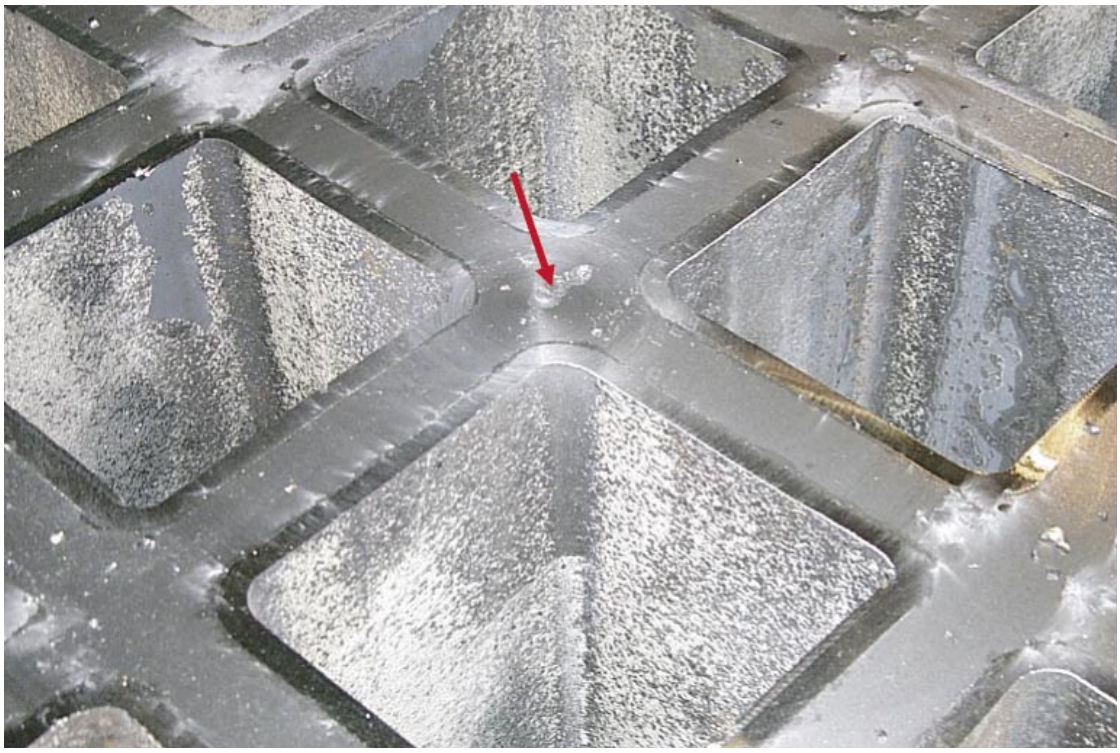

Figure 2-4. *Large casting defect observed on insert's cutting surface for Mock-up #1.*

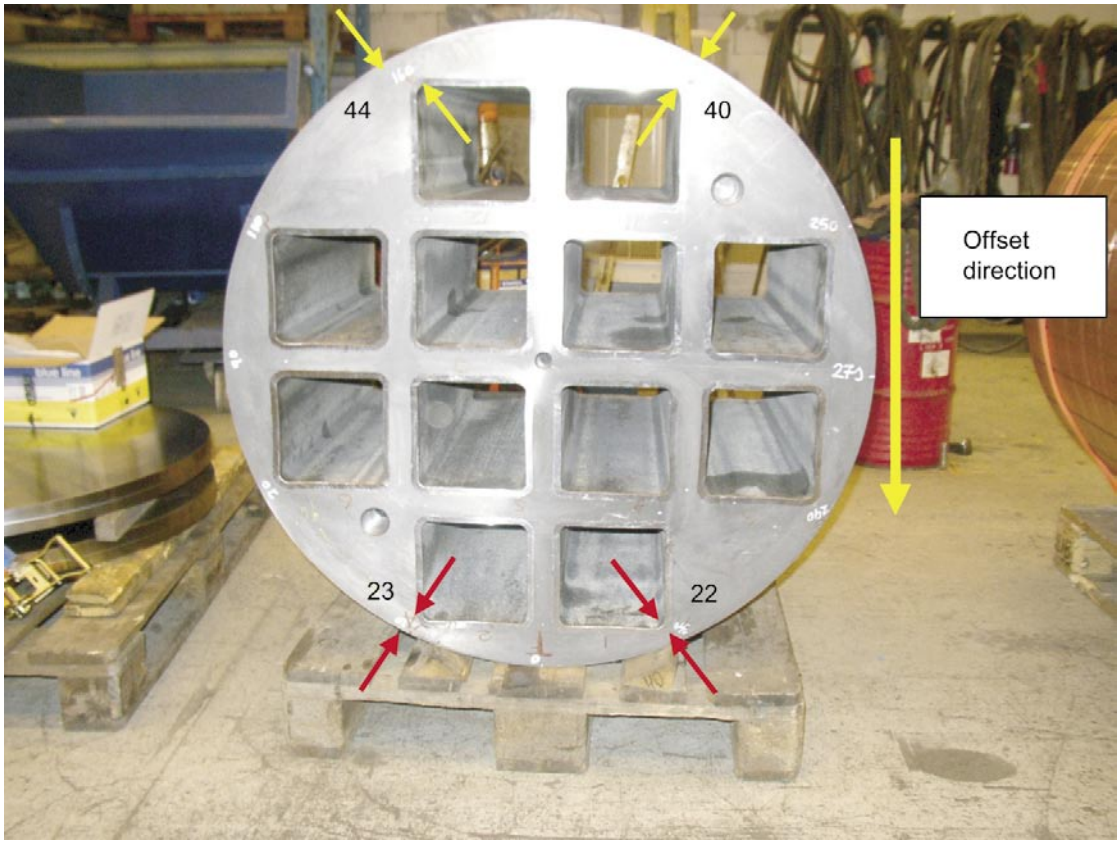

Figure 2-5. *Cross section of insert with variation in wall thickness indicated from fuel channel off-set.*

clearly result in an asymmetric load distribution and higher local stresses and deformation at the thinner side. In the probabilistic analysis /2/ this has been recognized as the most important factor for increasing the probability of canister failure at the design load.

The Mock-up #2 was cut from a segment of insert I24 with very small defect indications. Insert I26 had no fuel channel off-set but instead the corner radius of the steel cassette was smaller, (20–25 mm for I26 and 10–15 mm for I24, which gives a larger stress concentration at the corner. A small corner radius increases the computed probability for failure but it has a smaller effect than the off-set /2/.

3 Requirements for the isostatic pressure test

To perform the pressure test successfully a number of requirements were specified. Most importantly the press needed to be of sufficient size to allow testing of the large mock-up and the maximum load be sufficiently high to attain mock-up failure by fracture or plastic collapse. The yield stress decreases with higher temperature. The temperature for a canister in a future ice-age is expected to be 5–10°C. It was therefore also considered necessary that the temperature should not significantly exceed the room temperature since that would affect the onset of yielding. In addition, the applied pressure should be recorded, and if possible, the deformation should be measured during the test.

A cold isostatic press (CIP) of ASEA Quintus type at Schunk Kohlenstofftechnik in Heuchelheim, Germany, with inner diameter of 1,120 mm and height of 2,600 mm and maximum pressure 200 MPa was used in the tests. A cold isostatic press consists of a pressure vessel with a frame for axial support of the pressure vessel end closures and it uses water emulsion as the pressure medium as illustrated schematically in Figure 3-1. The pressure medium is pumped into the press. The hydraulic system of the press is designed to pressurize and decompress the pressure vessel in a controlled manner by means of an intensifier. Other presses were also considered but they did not fulfill the three basic test criteria (size, maximum load and temperature). The applied pressure was recorded on a PC-system with a sampling frequency of 0.5 Hz. It was not possible to directly measure the deformation during the loading, but sudden and local bulge-in, provided the leak-tightness remains intact, would be registered as small drop in the applied pressure. Simple elastic analyses indicate that a 1 MPa pressure drop would correspond to a bulge-in of around 1 litre. A complete failure of the mock-up would lead to complete de-pressurization, which would be registered from the pressure recording. The Mock-up #1 before a test cycle is shown in Figure 3-2a and Figure 3-2b shows the mock-up being placed into the press.

The same test procedure was adopted for all pressure cycles and both mock-ups. The mock-up was first loaded to a predefined maximum pressure, p_{max}. The maximum pressure was then kept for 120 seconds followed by a relatively rapid unloading. The mock-up was then taken out of the press and inspected visually. The residual plastic radial deflection was measured by means of a long steel ruler and vernier calipers where the steel ruler was pressed towards the stiff and straight upper part of the mockup as shown in Figure 3-3. The gap between the ruler and the mock-up was taken as the residual plastic deformation. The measurement procedure was repeated at several locations around the perimeter of the mock-up to determine the distribution of the residual deflection. The entire procedure was then repeated for a higher peak pressure.

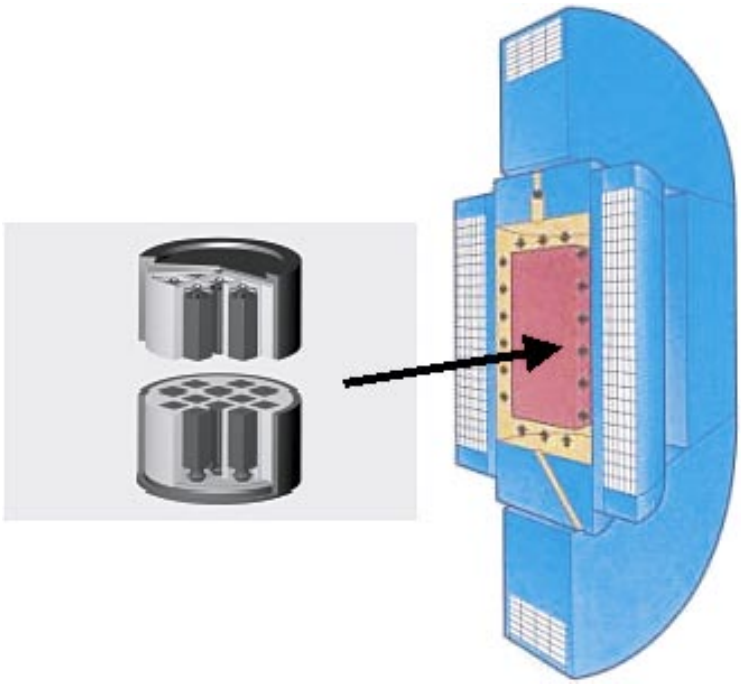

Figure 3-1. *Schematic illustration of the Quintus cold isostatic press (CIP) used in the test.*

a) *b)*

Figure 3-2. *a) Mock-up ready for testing b) mock-up inserted into the cold isostatic press.*

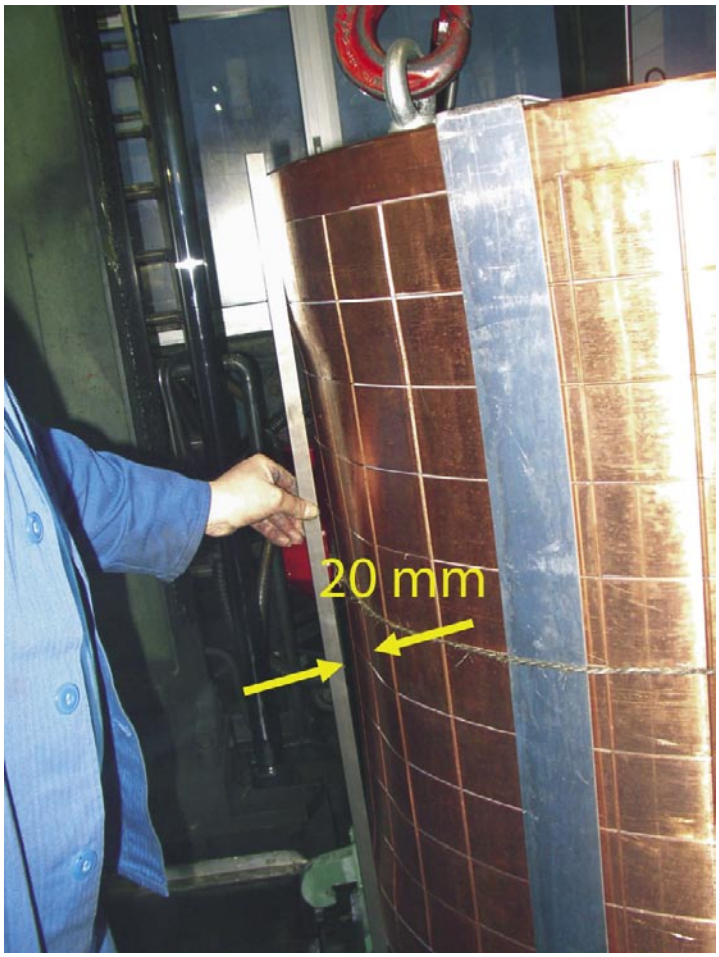

Figure 3-3. *Residual deformation of Mock-up #1 after pressure cycle with 130 MPa.*

4 Pre-test analysis

Three-dimensional elastic-plastic finite-element (FE) pre-test analyses were conducted by Ångpanneföreninen (ÅF)[2]. In the FE-model an earlier mock-up design with length 1,400 mm was used instead of 1,050 mm as in the final design. Some preliminary parameter studies showed that the maximum strain in the canister increases slightly with its length. For a canister with total length of 1,000 and 1,500 mm, the difference in maximum plastic strain and maximum effective stress in the insert was negligible as long as the deformation was elastic. At higher loads the values were slightly higher for the longer canister. For instance at p = 130 bar the maximum strain and effective stress were 11% and 479 MPa for the 1,000 mm insert and 14% and 519 MPa for the 1,500 mm insert. The FE-model therefore predicts slightly larger deformations than what would be expected for the tested mock-up. The finite element model of the mock-up with copper tube, copper lids, cast iron insert and steel plate is shown in Figure 4-1a and the insert is shown in Figure 4-1b. Due to symmetry assumptions only $1/8^{th}$ of the mock-up needs to be modelled for the FE-analysis. In the FE-analysis a yield stress and ultimate stress values of 350 MPa and 500 MPa respectively were adopted for the cast iron. These values are higher than those reported from the tensile tests of I26 (315 MPa and 400 MPa respectively) and I24 (260 MPa and 310 MPa) /5/. In compression there is more hardening but the relative difference between I24 and I26 was similar to what was observed for the tensile behaviour. The computed plastic deformation should be slightly underestimated, especially for the I24 insert. The copper was assumed to yield at 50 MPa and with low hardening behaviour (stress at 110 and 190 MPa for 4% and 20% strain respectively).

The stress concentration at the fuel channel corners can be clearly seen in Figure 4-2. The different colours represents values of the von Mises effective stress. Yielding occurs when the von Mises stress attains the yields stress. Figure 4-3a and 4-3b show the three principal stress directions and iso-contour values for the first principal stress at a pressure of 130 MPa. In the principal stress direction there are no shear stresses. The yellow/orange

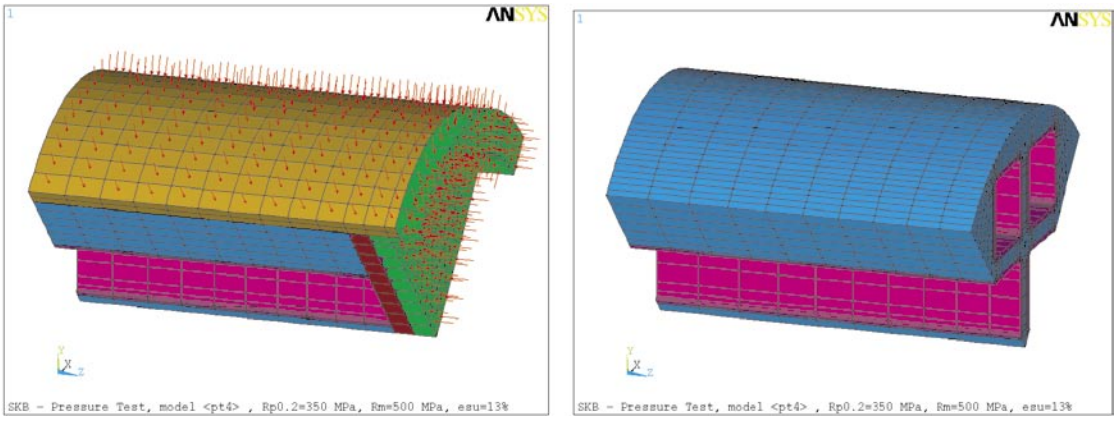

a) *b)*

Figure 4-1. *Finite element model of mock-up generated by ÅF a) entire mock-up with copper tube and lid, steel plate and tubes and cast iron insert b) cast iron insert. Blue cast iron insert, Purple = steel cassette, Orange = copper overpack, Green = copper lid, Brown = Steel lid.*

[2] The pre-test analyses presented in this report have been performed by Bo Erixon, Ångpanneföreningen and reported to K-F Nilsson by email.

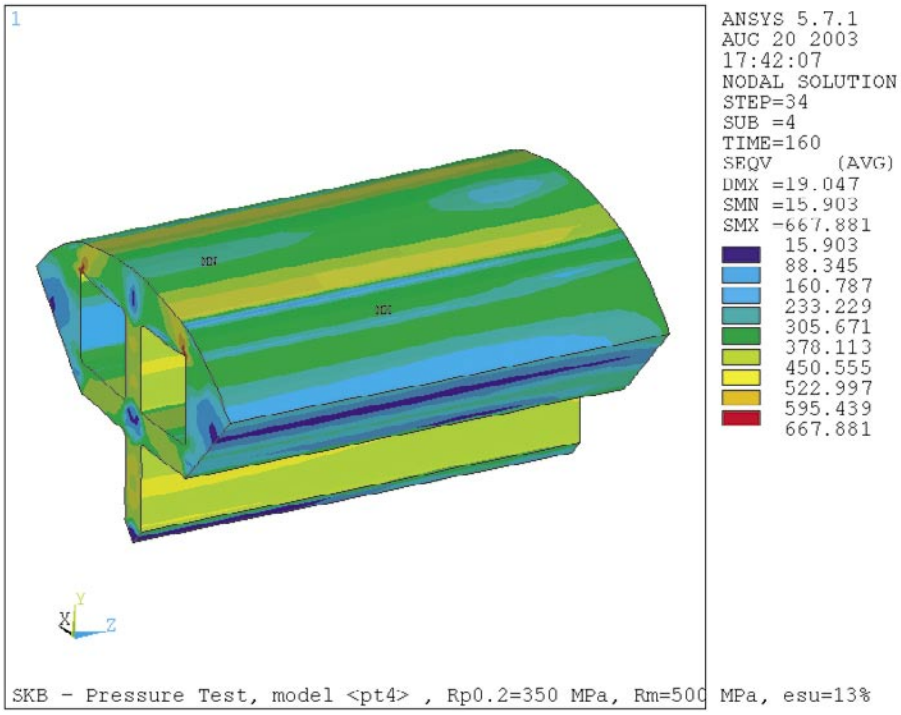

Figure 4-2. *Von Mises effective stress distribution in cast iron insert computed at p = 160 MPa. The different colours represent intervals for the von Mises stress.*

and red areas in Figure 4-3b represents the area with tensile stresses. For the "red" area the tensile stresses are above 387 MPa and that the material has yielded. The arrows in Figure 4-3a show the stress component tangential to the fuel channel surface, which is the one that can propagate cracks in the radial direction. Assuming that defects will only grow in tension loading, it follows that only defects in this region may become critical. Figure 4-4 shows the computed maximum plastic strain at the corner in the cast iron and the steel tube versus the applied pressure. The strains are larger in the steel tube but cracking in the steel tube is less critical than of the insert for the mock-up's overall integrity. The computed deformation versus the applied pressure is plotted in Figure 4-5 at the two locations indicated in the figure insert. The copper tube yields already below 10 MPa and the 2 mm gap between the tube and insert closes. The deformation then increases linearly until the insert yields at about p = 110 MPa, whereafter the plastic deformation increases rapidly. It is interesting to note that in the plastic regime the deformation is much higher in the 90° location than in the 45° location as defined by the figure insert, as the fuel channels introduce a loss of symmetry and the local wall thickness is much larger. It was mentioned above that the probabilistic analysis was based on local failure criteria, which is likely to be very conservative model for failure of the canister. This is illustrated by the von Mises iso-stress contours in Figure 4-6 (taken from /2/) where the red areas represent yielded material. The development of a local yielding can be seen at the corner of the insert already at a pressure of 44 MPa (Figure 4-6a), but it is not until a load of 130 MPa that a global failure mechanism is seen (Figure 4-6b). The results reproduced in Figure 4-6 were based on a two-dimensional model of the insert and without the copper overpack, which gives somewhat lower loads for local and global yielding. In addition, global plastic collapse could be lower for a model without double symmetry. Nevertheless the results give an idea of the margin between local and global plastic collapse. In /2/ the measured compressive stress-strain data from the three inserts was used, which was a bit lower than what was used in the "pre-test" analyses.

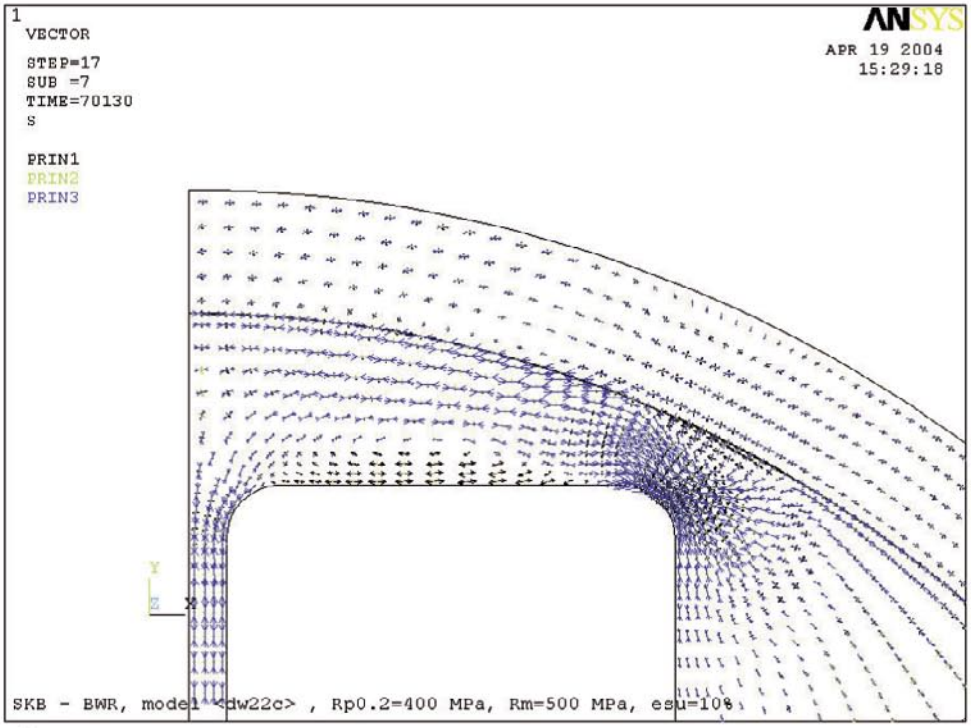

a)

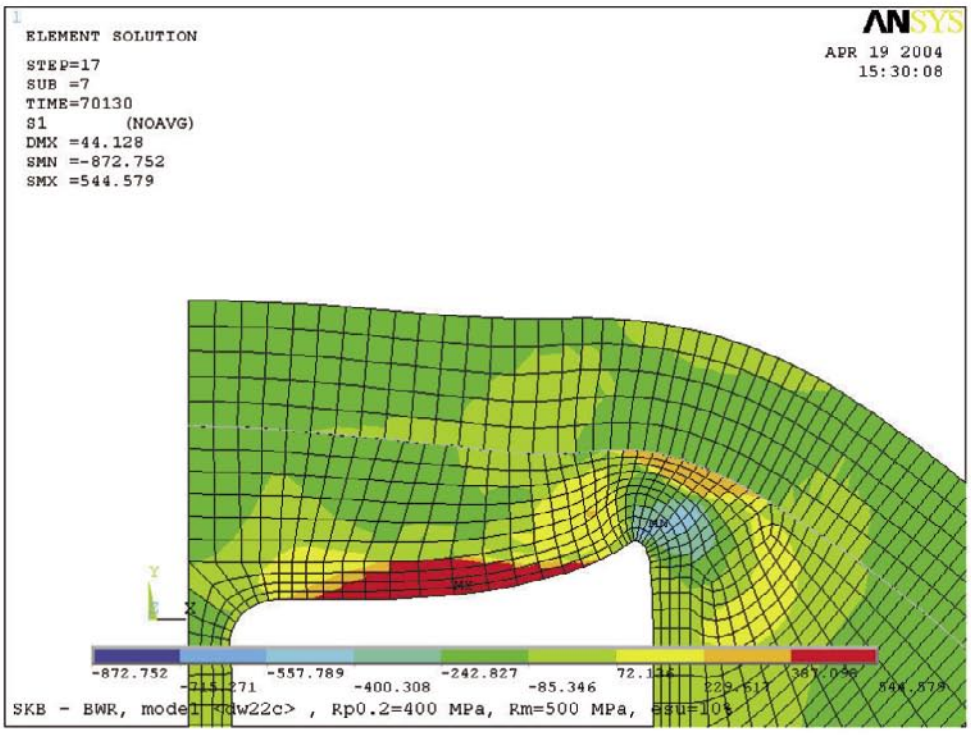

b)

Figure 4-3. *The distribution of a) the direction of principal stresses b) iso-stress contours for tangential stress component. The red surface indicates that the stress is above 350 MPa and the material has essentially yielded.*

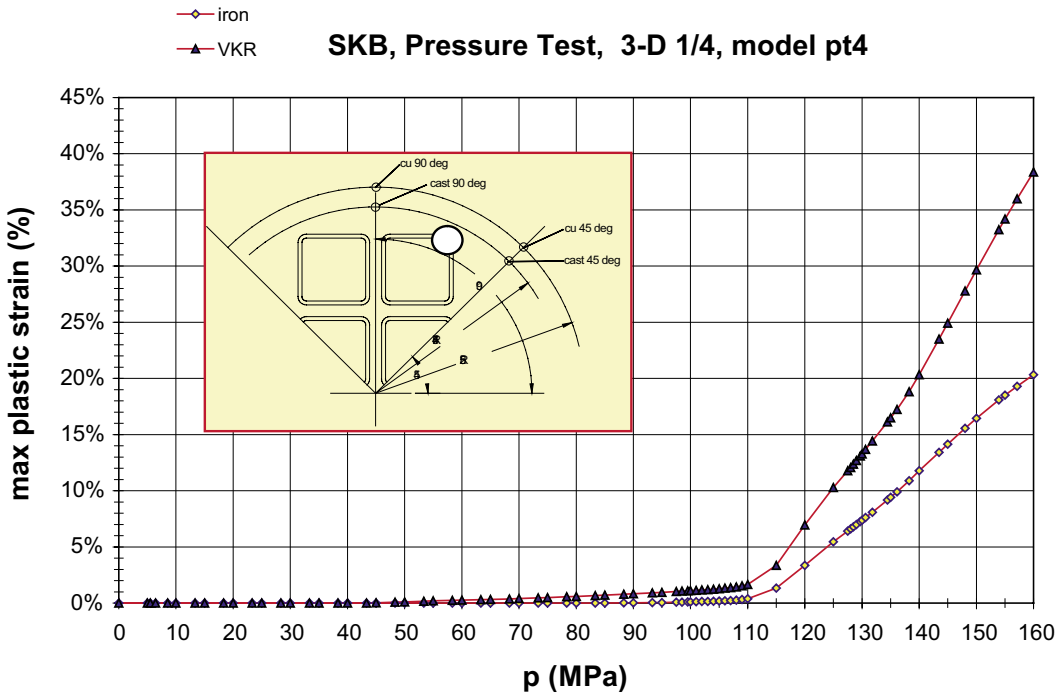

Figure 4-4. *Computed plastic strain versus applied pressure at corner of the channel in steel tube and insert respectively. The white circle indicates the location where the largest strains are computed.*

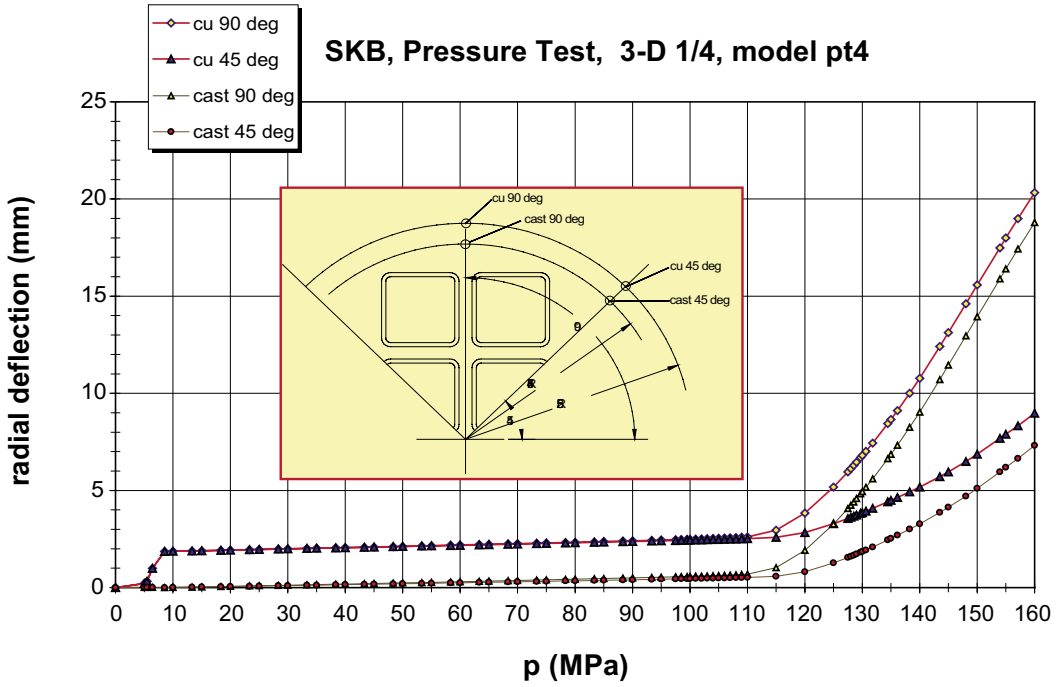

Figure 4-5. *Computed radial displacement in copper and insert at the reference points.*

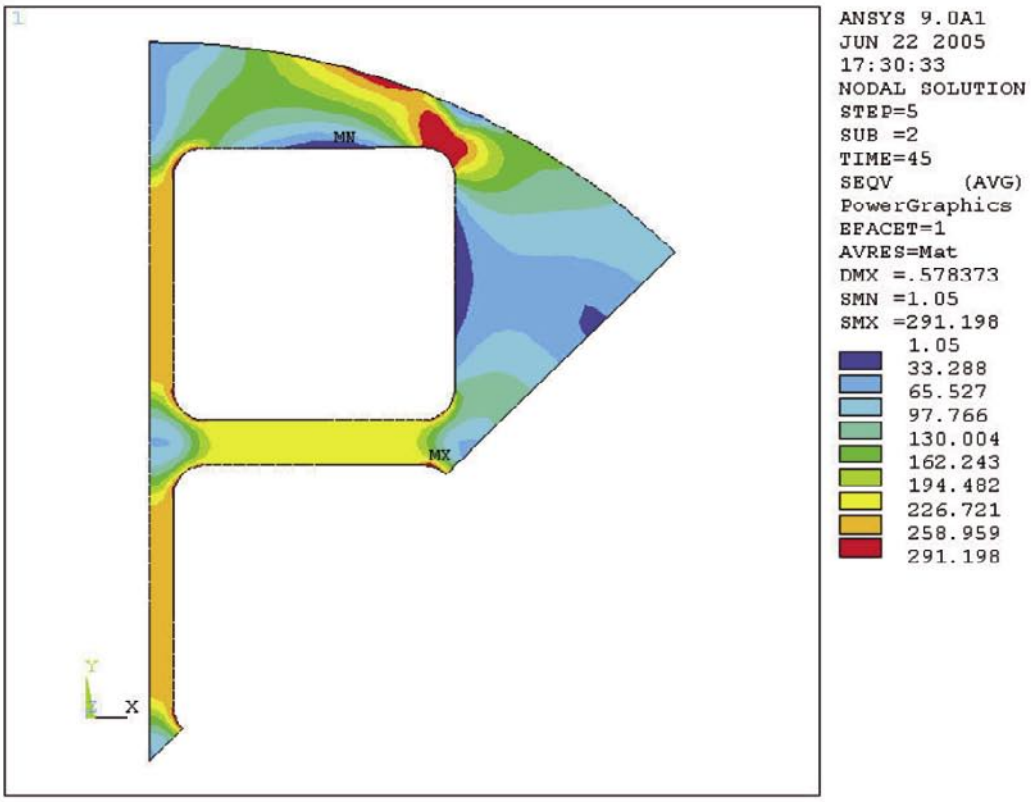

a)

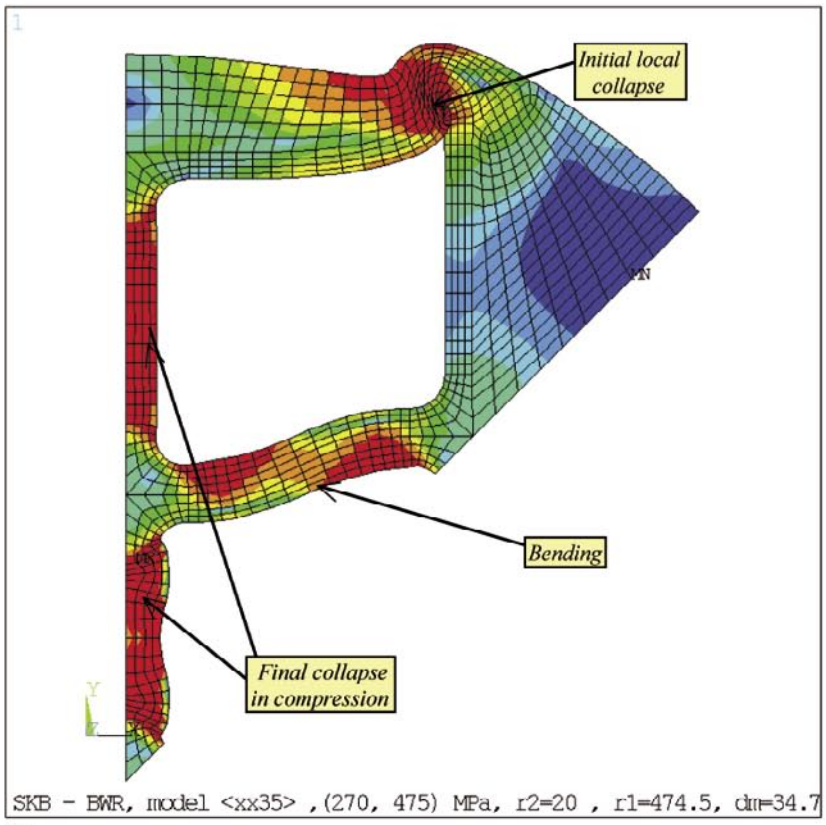

b)

Figure 4-6. *Computed von Mises effective stresses for 2D-FE model without copper over-pack a) local plastic stress concentration at corner of fuel channel at p = 44 MPa b) final collapse geometry at p = 130 MPa /2/.*

5 Test results

5.1 Mock-up #1 with insert from I26

Four load cycles were performed with p_{max} = 40, 70, 100 and 130 MPa respectively as specified in Table 5-1. The applied pressure history is plotted in Figure 5-1 for the first and final load cycle. At 30 MPa the higher pressure amplifier with lower pump capacity is activated which seen as a reduction in the pressure rate (pressure increase per second) in the figure.

Table 5-1. Summary of load cycles and main observations.

Pressure cycle	p_{max} (MPa)	Time (ramp+hold) (s)	Observation
1	40	120+120	Copper tube deformed plastically corresponding to closure of 2 mm gap between insert and tube.
2	70	320+120	As in Pressure cycle 1.
3	100	530+120	Onset of plastic deformation of insert. Residual radial deformation up to 5 mm.
4	130	500+120	Large plastic deformations with residual radial deformation up to 20 mm. CIP pumping fluid into press during hold time indicating time dependent deformation.

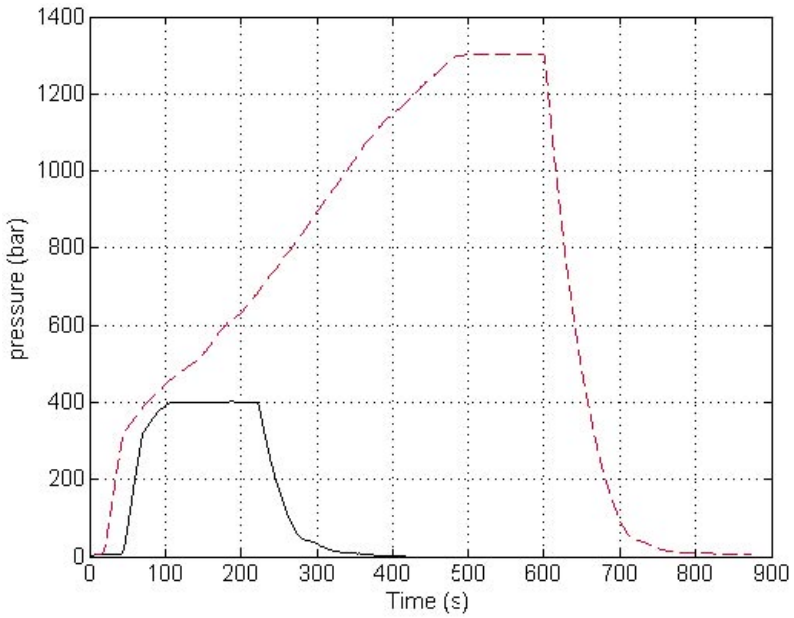

Figure 5-1. *Applied pressure cycles for Mock-up #1 with p_{max} = 40 MPa and 130 MPa.*

After the 40 MPa load cycle the deformation from 0.5 to 2 mm was measured using the simple measurement procedure outlined above. These values are in excellent agreement with the FE predictions in Figure 4-4 to 4-5 and correspond to the closure of the gap between the insert and the tube. The residual deformation after the 70 MPa was almost identical to what had been measured for the 40 MPa load cycle. This is also expected from the pre-test analysis because the insert is globally deformed elastically.

After the third load-cycle with p_{max} = 100 MPa, the measured residual deflection was almost 5 mm, which suggested that the insert had undergone plastic deformation. It can be seen from Figure 4-5 that this deflection is not predicted from the FE-analysis until a pressure of 125 MPa. The fact that plastic deformation in the test occurs at a lower load is probably mainly attributed the channel off-set but also to the higher yield and ultimate stress in the pre-test model.

In the final load cycle where p_{max} was increased to 130 MPa, the maximum residual radial deflection was measured to 20 mm, which corresponds to the computed deflection at 160 MPa. Figure 3-3 shows the measurement after the final load cycle. The maximum plastic deformation occurred at the location where the wall has the minimum wall thickness. The overall plastic deformation was quite non-symmetric and was only a few millimetres where the wall was thicker. The mock-up was still functioning, i.e. its leak-tightness was still intact. No pressure drop, indicating a sudden local bulge-in, was recorded during the loading as can be seen from Figure 5-1. During the 120 second hold period, there appeared to be a sound of active pumps. This indicated that the press needed to pump in some extra fluid to retain the pressure, which in turn points to some time dependent deformation. During the test, the pressure is forced to follow the prescribed history but the actual volume that is pumped into the press is not monitored. The time dependent deformation could therefore not be verified by recorded data. Leakage was ruled out as an explanation as the extreme pressure difference would mean that the O-rings were not functioning, but this would have lead to fast decompression. The load was not further increased since we wanted to investigate whether there had been any growth of defects as described in detail below. The insert with the local indented “ridge” is shown in Figure 5-2a. The steel cassette had also debonded partly from the insert as seen in Figure 5-2b.

a) *b)*

Figure 5-2. *Insert of Mock-up #1 after pressure test showing a) indented ridge and b) debonding of steel cassette.*

5.2 Mock-up #2 with insert from I24

The pressure test of the second mock-up followed the same procedure and the main observations for each pressure cycle are summarized in Table 5-2. The observations up to p_{max} = 130 MPa were similar to those observed for Mock-up #1 but a small additional deformation was registered between 40–70 MPa and the deformation was more symmetric than for Mock-up #1. The purpose of the final load cycle was to load the mock-up until failure. At 139 MPa, a loud bang could be heard, the pressure dropped almost instantaneously and the test was immediately stopped. The deformed mock-up when it is being lifted out of the CIP is shown in Figure 5-3. The deformation after the collapse was quite non-symmetric with a maximum indentation of almost 200 mm. The large deformation also induced large cracks in the upper part of the copper over-pack, as also illustrated in Figure 5-3 and pressure medium could enter the canister, which resulted in the fast pressure drop. The large deformation of the insert and copper shell are also shown in Figure 5-4. The failure mode is clearly global plastic collapse.

Figure 5-5 shows the minimum and maximum residual deformation measured along centre of the two mock-ups. We see that the difference between the minimum and maximum deformation, which is an indication of the asymmetry, is much larger for Mock-up #1 than for Mock-Up #2. The onset of large plastic deformations when the pressure exceeds 100 MPa are also clearly seen. The lower values for onset of plasticity compared to the analyses is probably due to the off-set in Mock-up #1 and lower yield stress and hardening for Mock-up #1 and #2.

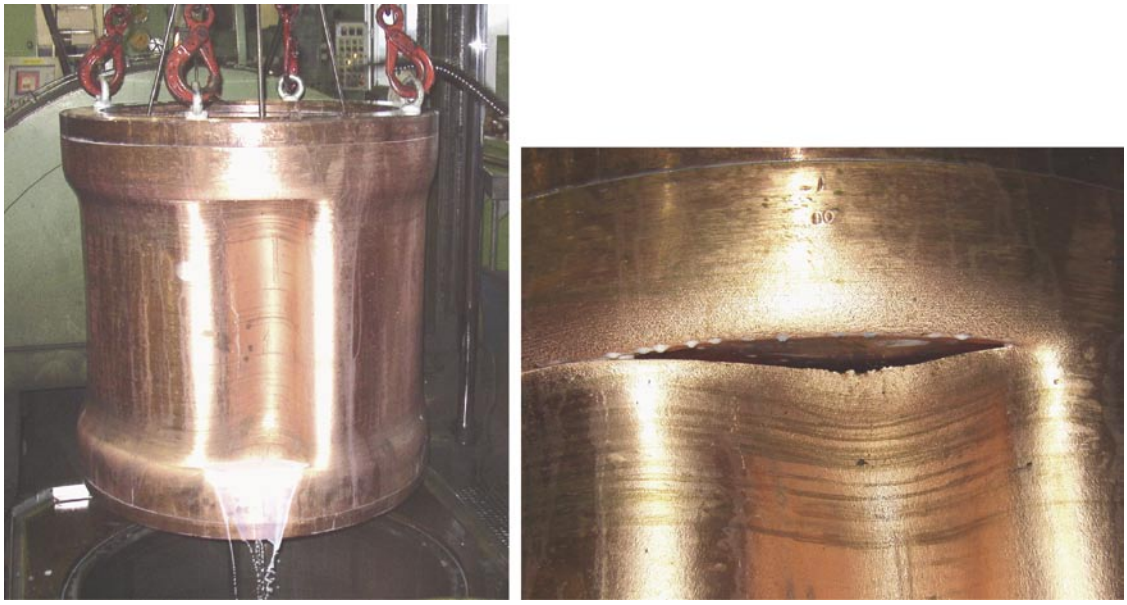

a) *b)*

Figure 5-3. *a) Mock-up #2 after loading to 139 MPa b) detail of severed copper over-pack at steel plate.*

Table 5-2. Summary of load cycles and main observations.

Pressure cycle	p_{max} (MPa)	Time (ramp+hold) (s)	Observation
1	40	50+120	Copper tube deformed plastically corresponding to closure of 2 mm gap between insert and tube.
2	70	90+120	Some plastic deformation up to 3.5 mm.
3	100	315+120	Onset of plastic deformation of insert. Residual radial deformation up to 4.5 mm.
4	130	400+120	Large plastic deformations with residual radial deformation varying from 11.5 mm to 4 around mock-up perimeter.
5	139	855	Large bang registered at p = 139 MPa with instantaneous pressure drop and test immediately stopped. A very large residual radial deformation of 195 mm at 90° marking.

a) *b)*

Figure 5-4. *Mock-up #2 showing large deformation after plastic collapse.*

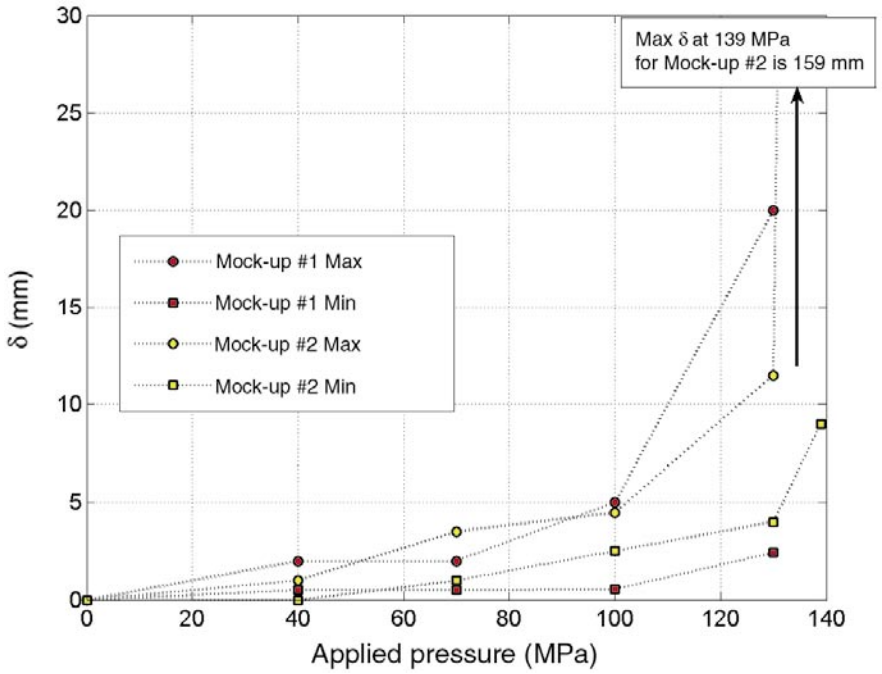

Figure 5-5. *Measured maximum and minimum residual radial deflection of Mock-up #1 and #2 versus applied pressure.*

6 Post-test analysis of Mock-up #1 to assess defect growth

The main purpose of the pressure test was to demonstrate safety margins against failure by plastic collapse or fracture. It is very difficult to state whether there was crack growth from the measured relation between applied load and residual deformation. The Mock-up #2 clearly failed by plastic collapse. The pressure test for Mock-Up #1 was stopped before plastic collapse had been attained in order to investigate in more detail possible crack growth. The computed failure probabilities in /2/ are based on local plastic collapse in the corner region and initiation of crack propagation. This is a quite conservative assumption since the canister is not expected to fail until there is a "global" failure mode as outlined in Figure 1-3. In the plastic failure case, the Mock-Up tests clearly show that the canister can sustain the local yielding (which occurs at 45–60 MPa according to analyses /2/ and shown in Figure 4-6a) whereas global plastic collapse occurs above 130 MPa, which is in excellent agreement with the predictions in Figure 4-6b. A similar safety margin is expected for the computed "fracture mode" (illustrated schematically in Figure 1-3 by difference for onset of stable tearing and final fracture). Figures 6-1a–d give a schematic illustration of possible scenarios for crack propagation. To start with there must be a defect of sufficient size in the tensile region (Figure 6-1a). It is very likely that the ligament between the crack and the free surface would break as illustrated in Figure 6-1b. But even in that case initiation of crack propagation from slag defects is not expected to lead to canister failure for two reasons: i) cracks are expected to have stable tearing due the material's crack growth resistance (Figure 6-2) and ii) cracks that initiate in the tensile region must propagate through a compressive region before it can become a through-wall crack. The most likely scenario is then that the crack would arrest at a certain depth (Figure 6-1d). However, as a result of crack advance, stresses will be redistributed and one could imagine a situation where the tensile stresses move with the crack tip as outlined in Figure 6-1c. This scenario in combination with low crack growth resistance could potentially lead to fracture. To compute to what extent the stresses redistribute would, however, require an analysis with the crack growth explicitly modelled.

To assess which scenario that happened a step-wise post-test analysis programme was implemented. To demonstrate the intrinsic safety of the design, it is better if we can show that there was some crack growth and arrest, since that would demonstrate inherent defect tolerance of the design. Mock-up #1 was first inspected for any surface breaking defects using dye-penetrant technique. The dye penetrant indicated presence of surface cracks in the indented region as indicated in Figure 6-3 but it was not possible to inspect the inside of the fuel channels because of partly bonded steel cassettes. The insert was then cut into smaller segments as illustrated in Figure 6-4. The segments L1–L3 and R1 and R2 were all taken from the region with the smallest wall thickness since the stresses, and therefore the likelihood for crack propagation was highest there. All segments were first inspected by radiography to localize and size cracks using accelerating voltage of 420 kV with conventional Philips X-ray source and 1–3 MeV linear accelerator (Linatron) (Figure 6-5a)[3]. Figure 6-5b shows radiography of L1 segment with the surface-breaking cracks at the inner surface of one fuel channel in the region with the maximum tensile stresses (see arrows). All cracks were in the axial direction. The largest number of defects

[3] L Metten, Radiographic inspection of KBS-3 canister mock-up Ref: hfr/lm/lm/0410.029 D(04)22128.

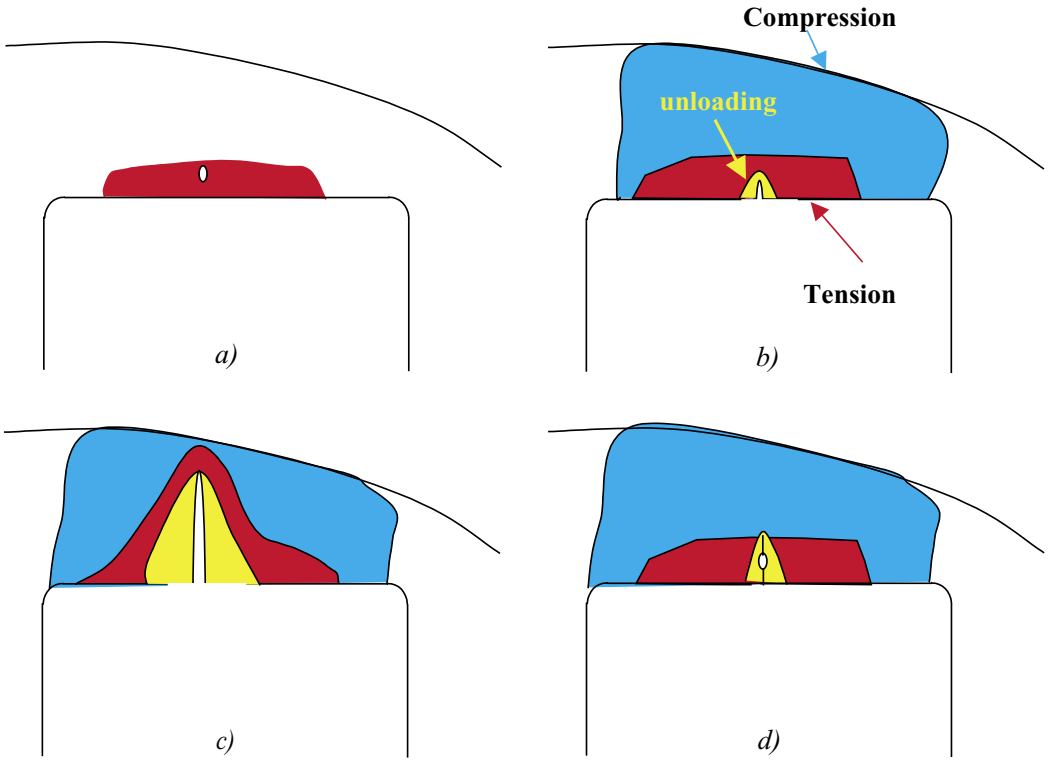

Figure 6-1. *Schematic illustration of potential scenario of for crack propagation a) defect in tensile region b) defects propagates towards fuel element channel c) through wall propagation induced by load distribution from advancing crack and low crack growth resistance d) crack arrest as crack enters compressive region and minor load redistribution.*

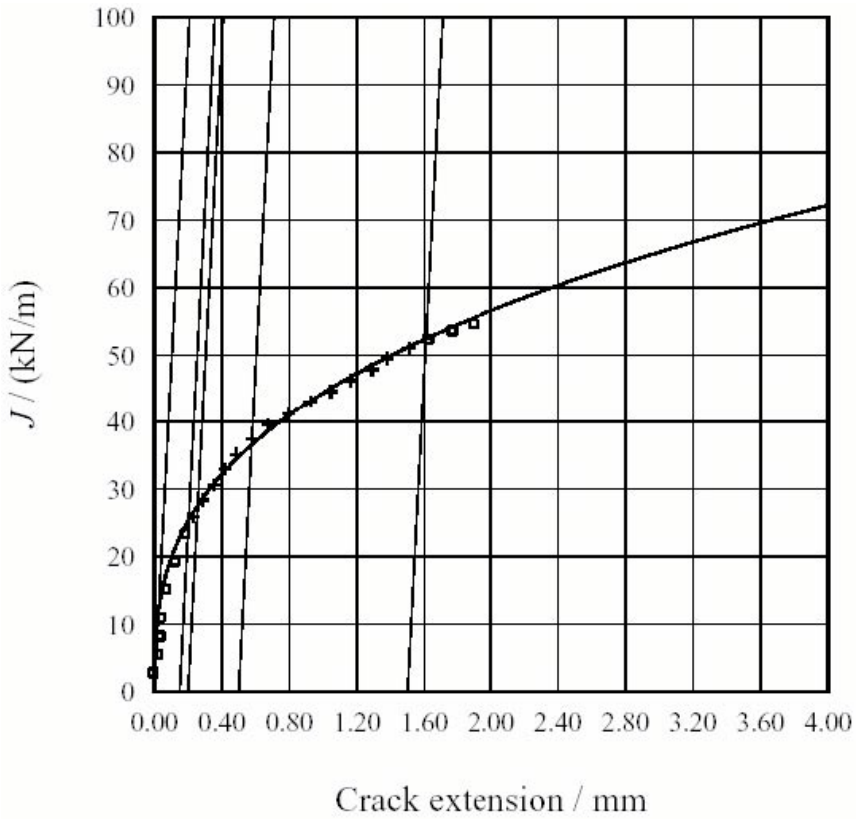

Figure 6-2. *Example of a rising J – Δa curve from one of fracture mechanics experiments at room temperature, J_{Ic} = 39 kN/m /7/.*

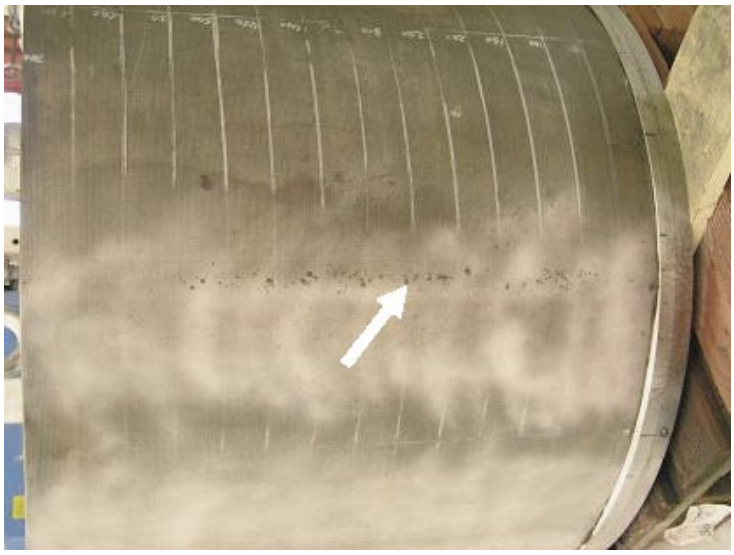

Figure 6-3. *Indication of micro-cracks in deformed region of Mock-up #1 by dye-penetrant.*

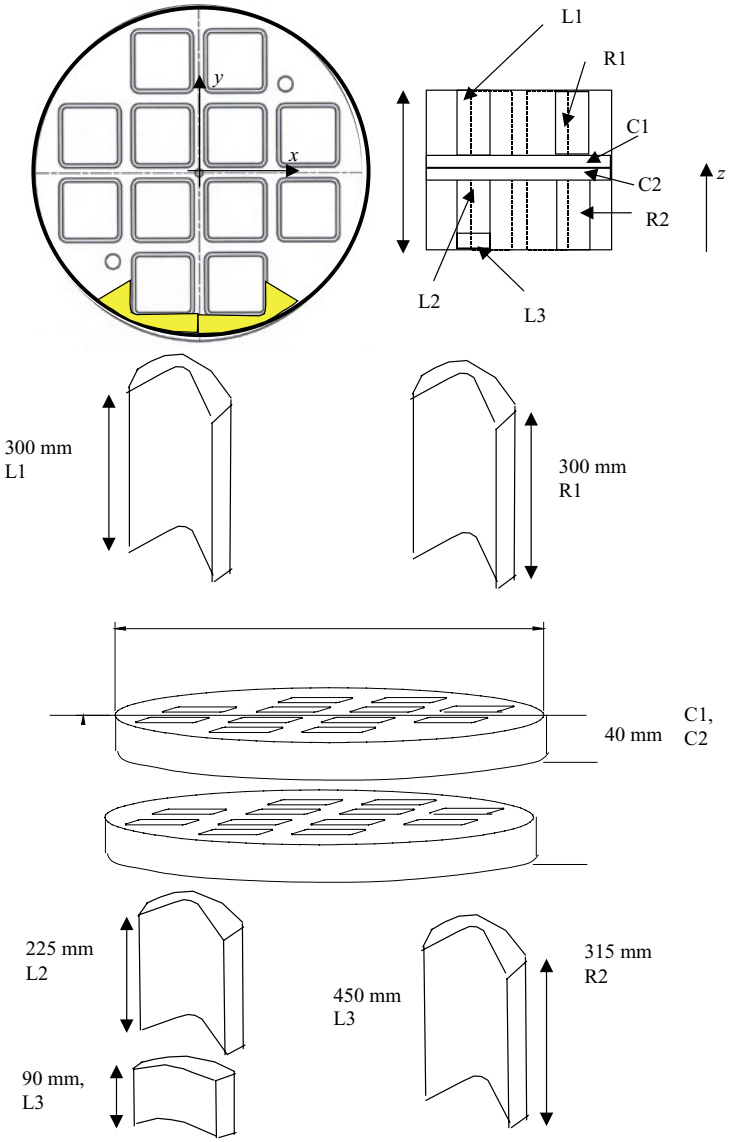

Figure 6-4. *Cutting scheme of Mock-up #1 for post-test analysis.*

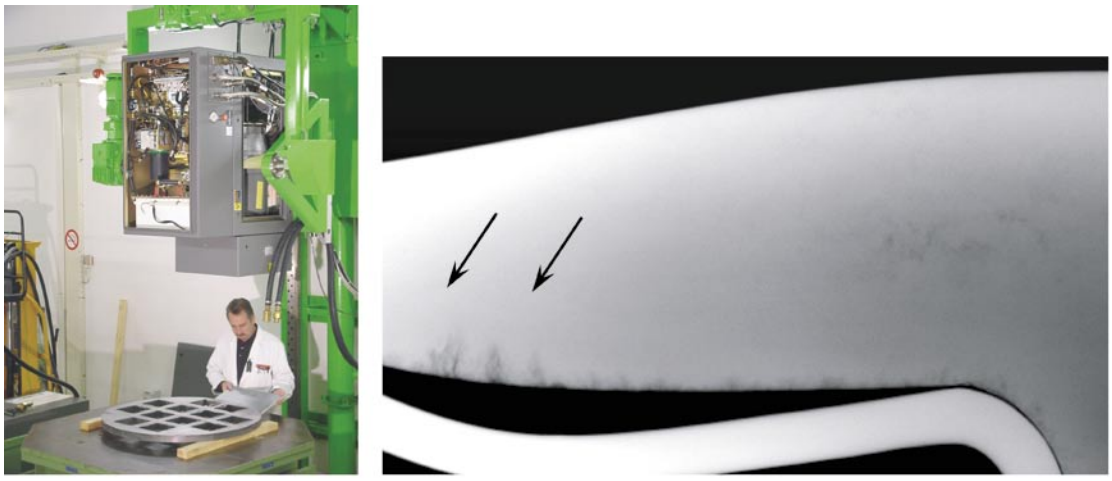

a) *b)*

Figure 6-5. *a) Radiography set-up with Linatron accelerator b) Radiography of L1 segment with surface breaking cracks at the interface with one of the steel fuel channels.*

(7) was detected in the segments L1 and L2 with maximum length of about 40 mm. However, radiography did not provide information about the crack depth and the crack propagation mode (tearing or cleavage). The segments L1 and L2 were therefore cut into smaller parts (Figure 6-6) to study the largest cracks in more details. The depth of the individual cracks in the "cut" pieces was measured with ultrasonic method in axial and tangential directions. Figure 6-7 shows a C-scan of two cracks in the "II part" of the L1 segment. The depths of these cracks in L1 and L2 were estimated to be about 10 mm, which corresponds roughly to the depth of the tensile region outlined in Figure 4-3b.

The smaller segments with cracks (e.g. cuts from II from L1 in Figure 6-6 and XX from L2) were polished and then broken open for metallographic and fractographic analyses, respectively as illustrated in Figure 6-8. The lower part of the piece was cut in thin slices that were polished and etched for metallographic inspections (Figure 6-8b). The fracture surface of one of the large cracks in L2 segment is shown in Figure 6-9. The measured crack depth is about 10 mm, which is in agreement with the ultra-sound measurement. The fracture surfaces were corroded.

Figure 6-10 shows details for one typical crack from segment L1 at the different magnifications. The crack profile suggests that it propagated by a stable tearing mechanism. Details of the crack tip morphology in Figure 6-10b–d indicate that crack grew first by stretching the material directly ahead of the crack tip. The graphite nodules then debonded from the matrix forming a void elongated in the direction perpendicular to the crack plane. Subsequent tensile deformation of the ligaments of the remaining matrix between the voids resulted in their necking. Crack advance then occurred by coalescence of the voids with the crack tip when internal necks were torn apart (see Figure 6-10d). A similar crack morphology was found for the other cracks analysed with the same procedure.

The determination of crack initiation sites is more complex. The crack in Figure 6-10a was formed at the vicinity of a large subsurface inclusion. It is probable that this inclusion acted as a crack initiation site because no other suitable sites were observed at the surface. This assumption is supported by the analysis of the features observed in another defect in Figure 6-11.

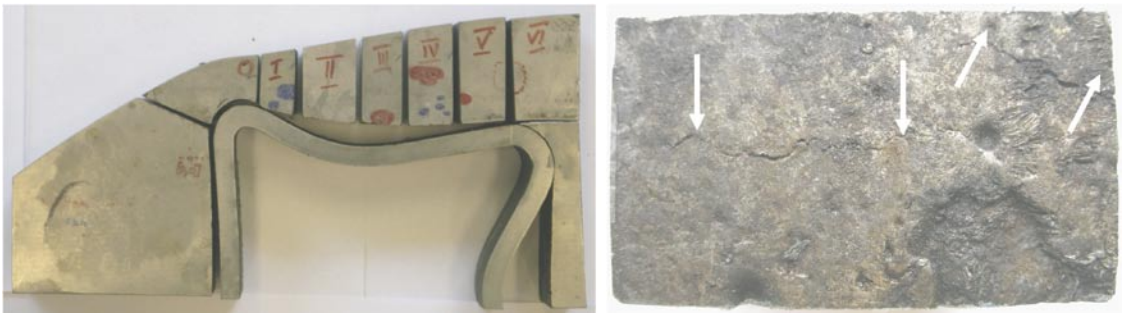

a) *b)*

Figure 6-6. *a) Segment L1 after cutting on smaller parts b) Two surface breaking cracks in part II in L1.*

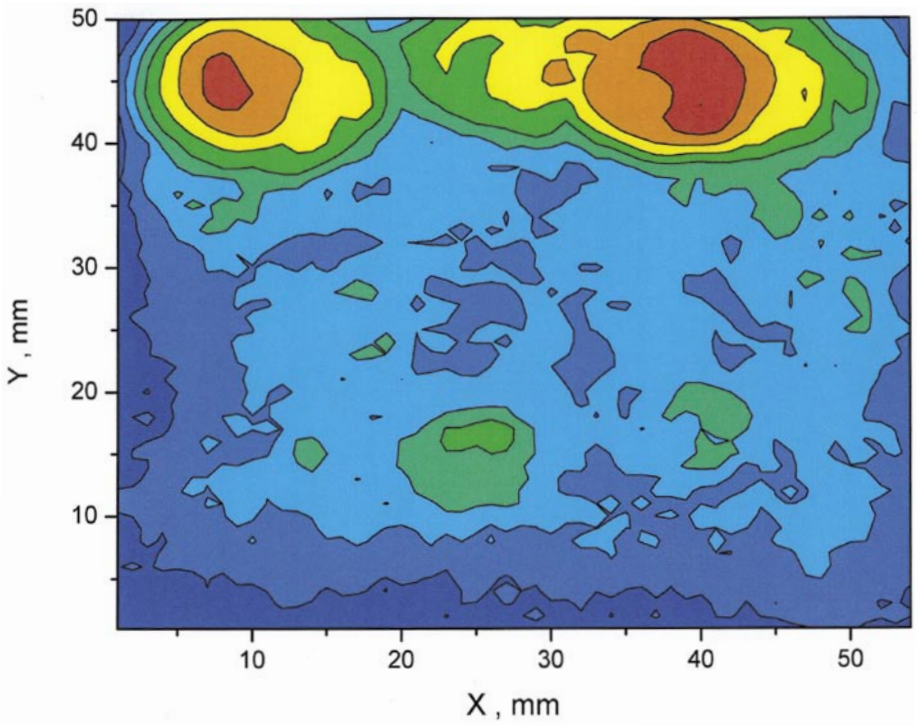

Figure 6-7. *C-scan of part II from L1 segment in tangential direction (perpendicular to the cracks) with two surface breaking cracks seen in Figure 6-6b. The different colours represent intervals for recorded echoes. Echoes below 6 dB contour (yellow, orange and red) line give a rough indication of the size of the defect.*

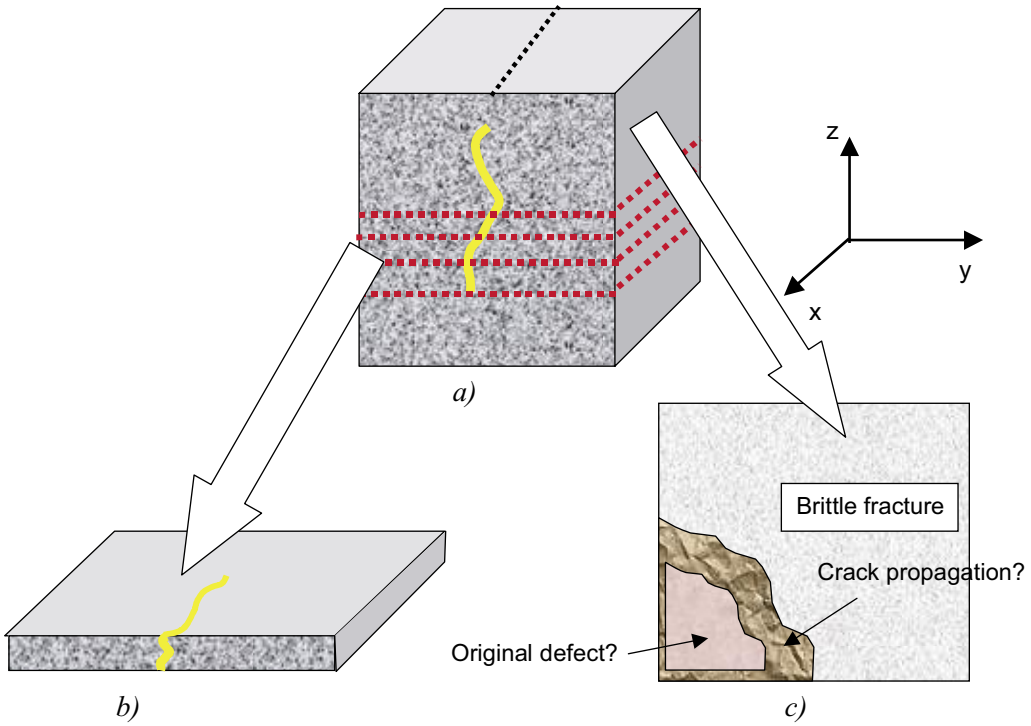

Figure 6-8. *Illustration of cutting of cracked segment a) segment with crack for investigation b)thin slices prepared from lower part of for metallographic investigation c) upper part broken open for fractography.*

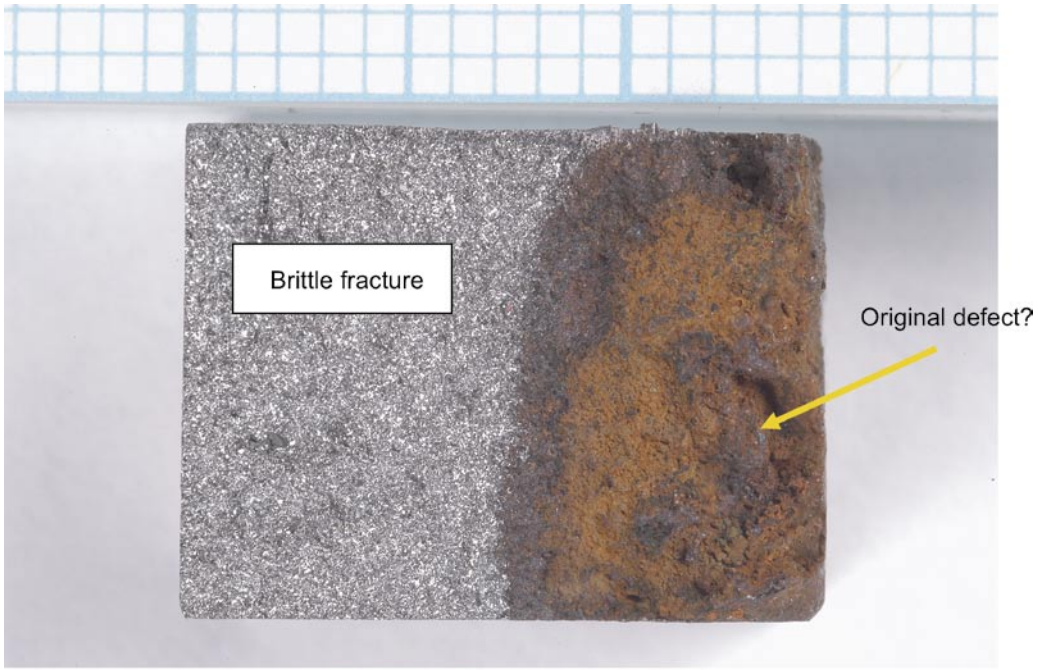

Figure 6-9. *Fractographic view of fracture surface showing surface with brittle fracture (grey area) from new crack surfaces from the opening of the cracked body and cracked area with oxidation.*

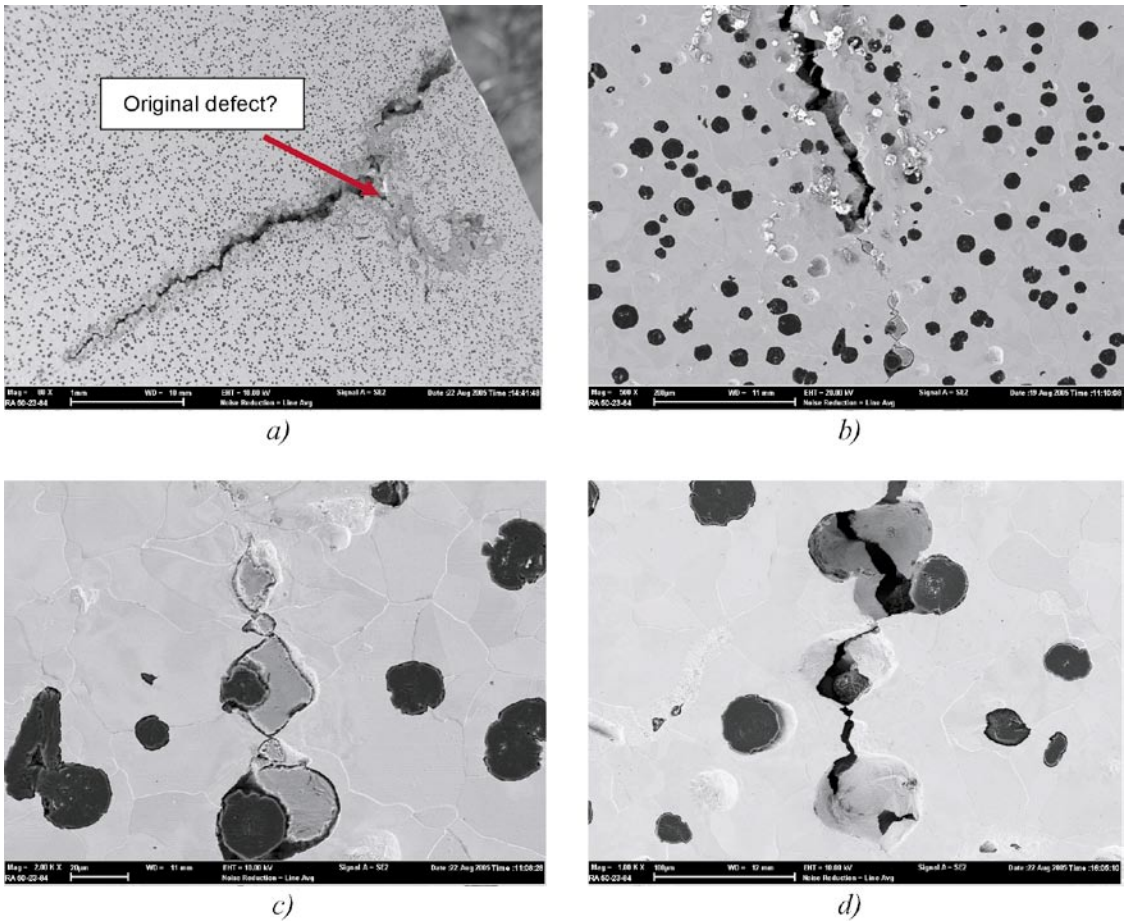

Figure 6-10. *Scanning electron micrographs of surface breaking crack from part II of L1 segment (see Figure 6-6) propagating in stable tearing shown at different magnifications a) entire crack b) magnification of crack tip with the voids ahead of the tip, c) void coalescence ahead of crack tip and d) detail of the void linking.*

Figure 6-11a shows a cross section of a peanut-shaped subsurface defect with the size of around 2.3×0.9 mm. Its smooth edges, which are partially or fully filled with the oxides (Figure 6-11b), suggest that it is a manufacturing defect. However, the broken ligament between the defect and surface exhibits quite different morphology. Here the cones of internal necking are clearly visible (Figure 6-11c). Obviously, the crack that connects the defect with the surface had to form under the influence of local tensile stresses in this zone. This illustrates the importance of large subsurface inclusion as crack initiators.

Another important issue for canister lifetime prediction is whether these cracks are pre-existing casting defects or formed during pressure tests. The defects without signs of internal necking are, obviously, manufacturing defects. However, it is not possible to determine unambiguously based only from the presence of the signs of local plastic deformation when cracks were formed. Local tensile stresses could develop and cause stable crack tearing induced by thermal stresses during cooling or mock-up testing. The presence of oxides in the crack is also not sufficient. Oxides could form during casting at high temperatures but also at room temperature due to water corrosion during sample preparation. Even the oxides in the “isolated” voids ahead of crack tip can be explained by corrosion. These voids are the part of a serrated 3 dimensional crack front and can be exposed to corrosion via paths, which are not visible on 2-dimensional cross sections. Thus, the assumption that cracks formed predominantly during mock-up testing is supported by the fact that they were found

only on the surface that was subjected to tensile stresses indicated by FEM analysis (see Figure 4-3). Despite numerous subsurface inclusions observed at the remaining sides of the fuel channels, cracks were absent there.

The cracks indicated in the zone of tensile stresses then propagated in stable tearing until it reached a dept of about 10 mm. There are two main reasons why the crack did not propagate further: 1) the stresses become compressive and the crack tip loading decreases 2) the material's rising crack growth resistance requires that the crack tip loading increases as the crack advances.

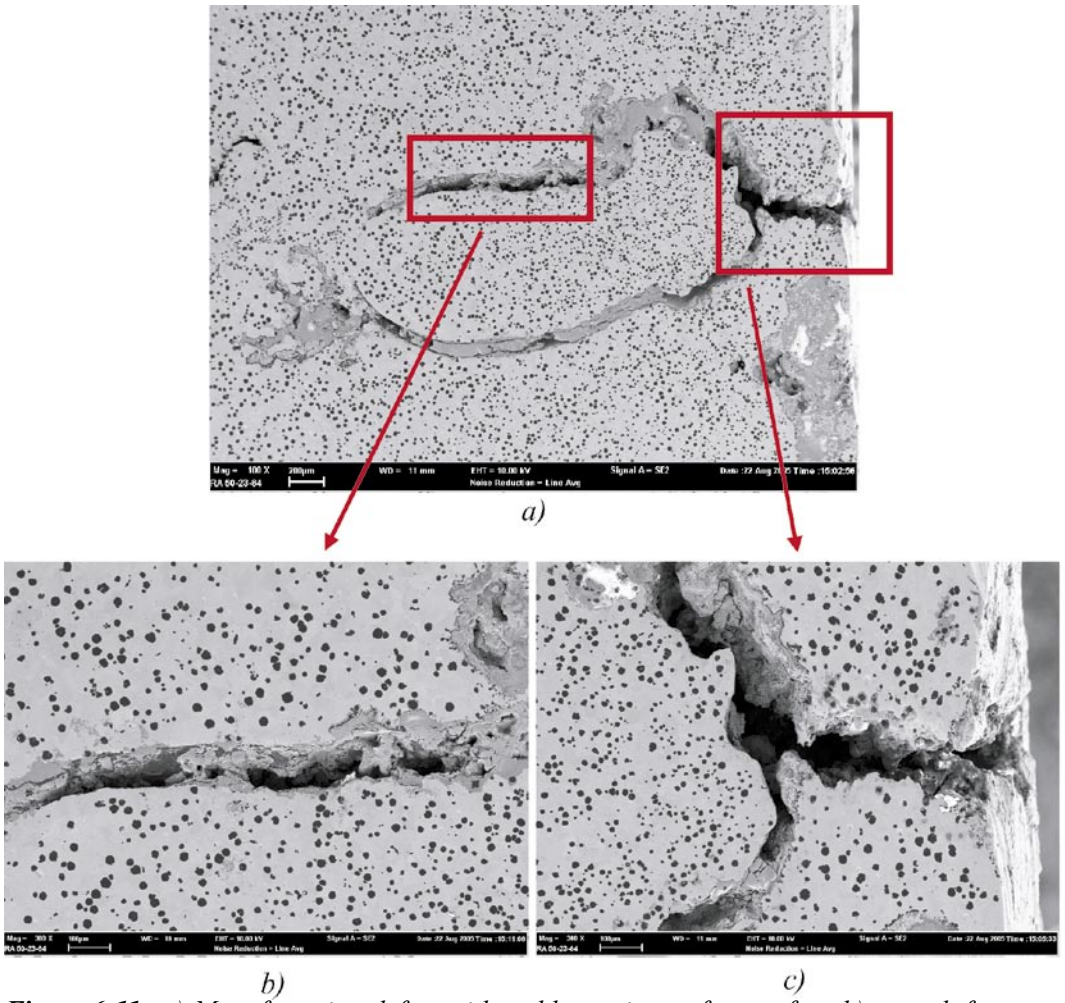

Figure 6-11. *a) Manufacturing defect with stable tearing to free surface b) smooth fracture surface for casting defect c) stable tearing serrated crack surface.*

7 Conclusions

Two large-scale pressure tests have been performed with a three-fold purpose: demonstrate the safety margin for a KBS-3 canister; to determine the failure load and associated mechanism; and to investigate the failure processes which have to be considered in the development of performance criteria and risk assessment of KBS-3 concept. The following main observations emerge:

- The design load for glaciation is 44 MPa. The mock-up remained intact up to a pressure of 130 MPa for both tests. The pressure test therefore clearly shows that the KBS-3 canister has large safety margins even for the extreme pressure that could occur during glaciation. This suggests that the iso-static load case can be ruled out as an event to be considered in an overall safety analysis of a KBS-3 repository system.
- The second mock-up was loaded until failure by plastic collapse, which occurred at a load of 139 MPa. This is in excellent agreement with two-dimensional finite element predictions.
- The defect tolerance of KBS-3 canister for the iso-static load was demonstrated by the pressure test and the post-test analysis of defects. Cracks are most probably initiated at the large subsurface inclusions in the zone of tensile stresses and grow by stable tearing. Further crack growth may be suppressed due to the crack growth resistance of the material and/or the fact that only a small region is actually in tension and cracks will arrest as they enter areas with compressive stresses.

Acknowledgement: We would like to acknowledge the contribution from Pietro Moretto (JRC) in the microstructural post-test analysis**.** The work by K-F Nilsson and F Lofaj was performed as part of the JRC-Action SAFECASK and funded by the European commission’s sixth framework programme.

References

/1/ **Werme L, 1998.** Design premises for canister for spent nuclear fuel, SKB TR-98-08, Svensk Kärnbränslehantering AB.

/2/ **Dillström P, 2005.** Probabilistic analysis of canister inserts for spent nuclear fuel, SKB TR-05-19, Svensk Kärnbränslehantering AB.

/3/ **Andersson C-G, 2002.** Development of fabrication technology for copper canisters with cast inserts, Status report in August 2001, SKB TR-02-07, Svensk Kärnbränslehantering AB.

/4/ **Andersson C-G, Eriksson P, Westman M, Emilsson G, 2004.** Status report, canister fabrication, SKB TR-04-23, Svensk Kärnbränslehantering AB.

/5/ **Minnebo P, 2004.** Statistical Analysis of Engineering Tensile Properties of Nuclear Waste Canister Insert Material, EUR21487EN, Joint Research Centre of the European Commission.

/6/ **Nilsson K-F, Andersson C-G, Nilsson F, Dillström P, Andersson M, Minnebo P, 2005.** A Probabilistic Methodology to Determine Acceptance Criteria and Failure Probabilities for the KBS-3 Ductile Cast Iron Inserts. In proceedings of MRS-05, 29th Symposium on the Scientific Basic for Nuclear Waste Management, Sep 2005, Gent Belgium, Material Research Society.

/7/ **Andersson C-G, Andersson M, Björkegren L-E, Dillström P, Erixon B, Minnebo P, Nilsson F, Nilsson K-F, 2005.** Probabilistic Analysis and Material Characterization of Canister Insert for Spent Nuclear Fuel – Summary Report, SKB TR-05-17, Svensk Kärnbränslehantering AB.

/8/ **Nilsson K-F, Blagoeva D, Moretto P, 2005.** Probabilistic fracture model to correlate failure strain with the microstructure of large cast iron components. Paper submitted for publication.

ISSN 1404-0344
CM Digitaltryck AB, Bromma, 2005